Electronic Journal of Biotechnology 78 (2025) 26–34

Contents lists available at ScienceDirect

Electronic Journal of Biotechnology

journal homepage: www.elsevier.com/locate/ejbt

Research article

Chufeng Yisun Decoction treats dry eye syndrome by inhibiting the PI3K/Akt pathway ☆

Yue Du [a,1], Xue Jiang [b,1], Yanyan Zhang [b], Quanyong Yi [b,*]

[a] Department of Pharmacy, Ningbo Eye Hospital, Wenzhou Medical University, Ningbo 315042, China
[b] Department of Ophthalmology, Ningbo Eye Hospital, Wenzhou Medical University, Ningbo 315042, China

GRAPHICAL ABSTRACT

Chufeng Yisun Decoction treat dry eye syndrome by inhibiting the PI3K/Akt pathway.

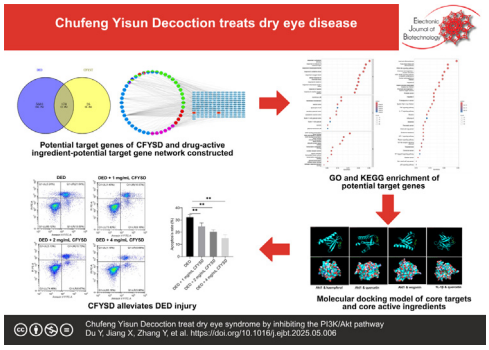

ARTICLE INFO

Article history:
Received 27 February 2025
Accepted 12 May 2025
Available online 13 August 2025

Keywords:
Active ingredients
Chinese medicine
Dry eye syndrome
Ekaempferol
HCE-T cells
IL-1β
Molecular docking
Network pharmacology
PI3K/Akt pathway
Quercetin
Wogonin

ABSTRACT

Background: Dry eye disease seriously affects people's work and life. Chufeng Yisun Decoction is a traditional Chinese medicine decoction used in treating dry eye disease. This study aims to explore the core active ingredients, targets, and mechanisms of CFYSD in dry eye disease, providing new insights for the dry eye disease treatment.
Results: A total of 196 target genes were screened from Chufeng Yisun Decoction, and 170 genes were related to dry eye disease. Gene Ontology and KEGG enrichment analyses showed that Chufeng Yisun Decoction influenced dry eye disease through "Lipid and atherosclerosis", "Fluid shear stress and atherosclerosis", and "PI3K-Akt". The core targets of Chufeng Yisun Decoction in treating dry eye disease were Akt1 and IL-1β. The core active ingredients were kaempferol, wogonin, and quercetin. Molecular docking results showed that the binding energies of kaempferol and Akt1, wogonin and Akt1, quercetin and Akt1, and quercetin and IL-1β were −6.1, −6.1, −6.1, and −7.9 kcal/mol, respectively. Chufeng Yisun Decoction significantly alleviated cell damage and reduced PI3K/Akt pathway-related protein expression.

☆ Audio abstract available in Supplementary material.

Peer review under responsibility of Pontificia Universidad Católica de Valparaíso.

* Corresponding author.
E-mail address: Quanyong_yii@163.com (Q. Yi).

[1] These authors contributed equally to this work.

https://doi.org/10.1016/j.ejbt.2025.05.006

PI3K activation partially reversed the therapeutic effect of Chufeng Yisun Decoction on dry eye disease. *Conclusions:* Chufeng Yisun Decoction treats dry eye disease by inactivating the PI3K/Akt pathway through multi-ingredients and multi-targets.

How to cite: Du Y, Jiang X, Zhang Y, et al. Chufeng Yisun Decoction treat dry eye syndrome by inhibiting the PI3K/Akt pathway. Electron J Biotechnol 2025;78. https://doi.org/10.1016/j.ejbt.2025.05.006.

1. Introduction

Dry eye disease (DED) is a multifactorial disease, primarily involving decreased lacrimal gland function, meibomian gland dysfunction, ocular surface inflammation, and corneal nerve dysfunction [1]. The prevalence of DED will continue to increase with the aging population, severely impacting visual function, professional work, and the quality of life of patients [2]. In DED patients, tear film imbalance induces an increase in tear osmolarity and leads to the release of inflammatory mediators such as interleukin (IL)-1β, tumor necrosis factor (TNF)-α, and IL-6, ultimately resulting in damage to the corneal and conjunctival epithelium [3]. Although inflammation has been recognized as a significant factor contributing to corneal epithelial changes and tear film instability in DED patients, the pathogenesis of DED has not been fully clarified [4]. Current treatment options mainly include artificial tears, anti-inflammatory agents, and antibiotics, but their safety and effectiveness are still under investigation [5]. Thus, it is imperative to develop new therapeutic approaches for DED.

In recent years, the therapeutic effect of Traditional Chinese Medicine (TCM) on DED has attracted increasing attention. Chufeng Yisun Decoction (CFYSD) is a famous TCM formula, composed of Rehmanniae Radix Praeparata, Angelicae Sinensis Radix, Paeonia Radix Alba, Chuanxiong Rhizoma, Ligustici Rhizoma Et Radix, Peucedani Radix, and Saposhnikoviae Radix. CFYSD has the functions of dispelling wind, clearing heat, nourishing blood, and promoting blood circulation. Both single herbs and compound formulations are widely confirmed to have the ability to alleviate symptoms of DED [6]. For instance, Achyranthis radix extract can restore tear secretion, maintain corneal smoothness, and reduce corneal epithelial apoptosis in DED [7]. In a DED mouse model, Modified Danzhi Xiaoyao Powder reduces the levels of TNF-α and IL-1β, promotes tear secretion, and repairs corneal damage [8]. The combination of Chi-Ju-Di-Huang-Wan and four-substance decoction significantly alleviates discomfort and inhibits tear vascular endothelial growth factor in patients with DED [9]. However, the therapeutic effect of CFYSD on DED and its underlying mechanism remain unclear.

The PI3K/AKT pathway plays a crucial role in corneal inflammation, epithelial proliferation, and corneal fibrosis in DED [10]. Inhibition of the PI3K/AKT pathway in DED can alleviate the inflammation levels in the cornea and conjunctiva, thereby exerting therapeutic effects [11]. Notably, natural compounds can alleviate DED by inhibiting the PI3K/AKT signaling pathway through multi-targets [12,13]. It remains unclear whether the PI3K/AKT pathway is involved in the therapeutic process of CFYSD in DED.

In this study, we investigated the mechanism of CFYSD in treating DED through network pharmacology analysis and experimental validation. Potential targets of CFYSD in treating DED were selected from databases. Gene Ontology (GO) and Kyoto Encyclopedia of Genes and Genomes (KEGG) enrichment analyses were conducted to explore the pathways enriched by potential targets. Finally, the mechanism of action of CFYSD on DED was validated at the cellular level.

2. Materials and methods

2.1. Identification of effective ingredients and target genes of CFYSD in treating DED

The TCMSP database (https://old.tcmsp-e.com/browse.php?qc=herbs) [14] was used to screen the effective active ingredients of CFYSD, including Rehmanniae Radix Praeparata, Angelicae Sinensis Radix, Paeonia Radix Alba, Chuanxiong Rhizoma, Ligustici Rhizoma Et Radix, Peucedani Radix, and Saposhnikoviae Radix, with the screening criteria set as oral bioavailability ≥ 30% and drug-likeness ≥ 0.18 [15,16,17]. Prediction of the target genes of these seven active ingredients was performed.

DED-related target genes were selected in GeneCards (https://www.genecards.org/) [18], OMIM (https://www.omim.org/) [19], and DrugBank (https://go.drugbank.com/) [20] databases. Subsequently, the intersection of the drugs and DED target genes was taken using a Venn diagram, and then, the candidate target genes for CFYSD in treating DED were obtained.

2.2. GO and KEGG enrichment analyses

The candidate target genes were subjected to GO and KEGG functional enrichment analysis using the "clusterprofiler" package in R language. During the enrichment analysis, a p-value < 0.05 was used as the criterion for selecting significantly enriched items. The GO functional terms and KEGG signaling pathways enriched with candidate genes were selected based on this criterion. The top 10 significantly enriched functional terms in Biological Process, Cell Component, and Molecular Function from GO enrichment, as well as the top 30 significantly enriched signaling pathways from KEGG enrichment, were visualized in the GO and KEGG enrichment plots.

2.3. Protein-protein interaction analysis and ingredients-target genes network construction

The candidate target genes were uploaded to the STRING database (https://cn.string-db.org/) [21] for protein–protein interaction analysis. The results were visualized using the cytohubba plugin in Cytoscape v3.8.0 software (Cytoscape Consortium, San Diego, CA, USA) to identify core targets. Additionally, Cytoscape v3.8.0 software (Cytoscape Consortium) was used to construct the active ingredient-target gene network diagram.

2.4. Molecular docking

Molecular docking was performed following the protocols described by Lu et al. [22] and Chen et al. [23]. The protein structure of the core target was downloaded from the PDB database (https://www.rcsb.org/) [24]. PyMol v2.40 software

(DeLano Scientific LLC, Palo Alto, CA, USA) [25,26] was used to remove water molecules and ligands from the structure. The structure of the core active ingredient was downloaded from the PubChem database (https://pubchem.ncbi.nlm.nih.gov/) [27]. The obtained PDB structures were converted to PDBQT format using AutoDockTools v1.5.6 (Scripps Research, La Jolla, CA, USA) to predict active pockets. Molecular docking predictions were performed using AutoDock Vina 1.1.2 (Scripps Research) [28], and the results were visualized with PyMol software.

2.5. Preparation of CFYSD

CFYSD consists of Rehmanniae Radix Praeparata, Angelicae Sinensis Radix, Paeonia Radix Alba, Chuanxiong Rhizoma, Ligustici Rhizoma Et Radix, Peucedani Radix, and Saposhnikoviae Radix, in a ratio of 1:1:1:1:1:1:1. The herbs were soaked in double-distilled water for 2 h, boiled for 1 h, filtered to obtain the liquid, and boiled again with water for 1 h. The two liquid mixtures were combined and filtered. The filtrate was then concentrated, frozen at −80°C overnight, lyophilized into powder, and stored for later use.

2.6. Cell culture and treatment

HCE-T cell lines purchased from Cellcook (CC4018, Cellcook, Guangzhou, China) were cultured in Dulbecco's modified Eagle medium (DMEM, 11320033, Thermo Fisher Scientific, Waltham, MA, USA) containing 10% fetal bovine serum (A5670701, Thermo Fisher Scientific), 10 ng/mL Epidermal growth factor (AF-100-15, Thermo Fisher Scientific) and 25 mM insulin (HY-P0035, MedChemExpress, Monmouth Junction, NJ, USA). The experiment included 6 groups: blank group (control), hypertonic induction group (DED), low-dose group (DED + 1 mg/mL CFYSD), medium-dose group (DED + 2 mg/mL CFYSD), high-dose group (DED + 4 mg/mL CFYSD), DED + 740 Y-P group/ DED + 4 mg/mL CFYSD + 740 Y-P group. Cells were cultured at 37°C in an incubator containing 5% CO_2.

NaCl was purchased from Thermo Fisher Scientific (AM9760G) at a storage concentration of 5 M. Before the experiment, NaCl was diluted to 90 mM with DMEM to simulate an osmolarity of 500 mOsm/L [29,30] and used to treat HCE-T cells for 48 h to establish the DED model. After the cells reached 80% confluence, the cells were treated with 20 μM 740 Y-P (HY-P0175, MedChemExpress) for 48 h and used for subsequent experiments.

2.7. Cell counting kit-8 (CCK-8) assay

Cell viability was determined using the CCK-8 kit (CK04, Dojindo Molecular Technologies, Tokyo, Japan). In brief, HCE-T cells were seeded in a 96-well plate and pre-incubated at 37°C for 24 h. Cells were exposed to hypertonic solution and different concentrations of CFYSD (0.25, 0.5, 1, 2, 4 mg/mL) for 12, 24, and 48 h, and the DED model was treated with different concentrations of CFYSD (0.25, 0.5, 1, 2, 4 mg/mL) for 12, 24, and 48 h, with blank group as control. The above cells were incubated with 10 μL of CCK-8 solution for 1 h, and the absorbance at 450 nm was measured.

2.8. Flow cytometry analysis

HCE-T cells in logarithmic growth phase were seeded into a 96-well plate and treated according to experimental groupings for 48 h. After washing the cells, cell apoptosis was detected using the Annexin V-APC/PI Apoptosis Kit (E-CK-A217, Elabscience, Wuhan, China), followed by flow cytometry analysis using BD FACS Canto (Becton, Dickinson and Company, Franklin Lakes, NJ, USA).

2.9. Enzyme-linked immunosorbent assay (ELISA)

The supernatant was collected from cell cultures of each group, followed by detection of the levels of IL-1β and TNF-α according to the instructions of the kit (EKF57064/EKF57120, Biomatik, Kitchener, Canada).

2.10. Western blot assay

Cells were lysed using radioimmunoprecipitation assay lysis buffer (Wuhan Boster Biological Technology, Wuhan, China), and the protein concentration was determined using a bicinchoninic acid kit (AR1189, Wuhan Boster Biological Technology). Afterwards, proteins were separated using sodium dodecyl sulfate polyacrylamide gel electrophoresis (20 μg) and then transferred to a polyvinylidene fluoride membrane (Immobilon-P, Merck Millipore, Darmstadt, Germany). The membrane was blocked with 5% bovine serum albumin at room temperature for 1 h and washed with Tris-buffered saline with 0.1% Tween 20 (TBST). Subsequently, the membrane was incubated overnight at 4°C with primary antibodies including rabbit monoclonal anti-Akt (#4691, 1:1000, Cell Signaling Technology, Danvers, MA, USA), rabbit monoclonal anti-p-Akt (#2965, 1:1000, Cell Signaling Technology), rabbit polyclonal anti-PI3K (#4292, 1:1000, Cell Signaling Technology), rabbit polyclonal anti-p-PI3K (#4228, 1:1000, Cell Signaling Technology), and rabbit polyclonal anti-β-Actin (#4967, 1:1000, Cell Signaling Technology). After TBST wash, the membrane was incubated with goat anti-rabbit immunoglobulin G (IgG) secondary antibody (ab205718, 1:2000, Abcam, Cambridge, UK). Following another round of washing, the bands were visualized using an enhanced chemiluminescence kit (ABS920, Absin, Shanghai, China), and the gray values of band were analyzed using ImageJ software.

2.11. Statistical analysis

Statistical analysis and data graphing were performed using SPSS 21.0 software (IBM, Armonk, NY, USA) and GraphPad Prism 8.0 software (GraphPad Software Inc., San Diego, CA, USA). Continuous data were presented as mean ± standard deviation. First, normality and homogeneity of variance tests were conducted, which verified that the data were in normal distribution and homogeneity of variance. Comparison between groups was analyzed using *t*-tests, one-way analysis of variance (ANOVA), or two-way ANOVA, followed by Tukey's multiple comparisons test. *p*-values were obtained from two-tailed tests, with $p < 0.05$ considered statistically significant.

3. Results

3.1. Screening and enrichment analysis of target genes for CFYSD in treating DED

To identify potential targets for CFYSD in the treatment of DED, the effective ingredients and potential target genes in CFYSD were predicted using the TCSMP database. A total of 882 target genes were obtained (Table S1). After removing duplicate target genes, 196 target genes were retained. Subsequently, the GeneCards, OMIM, and DrugBank databases predicted DED-related target genes, and after removing duplicates, a total of 5853 DED-related

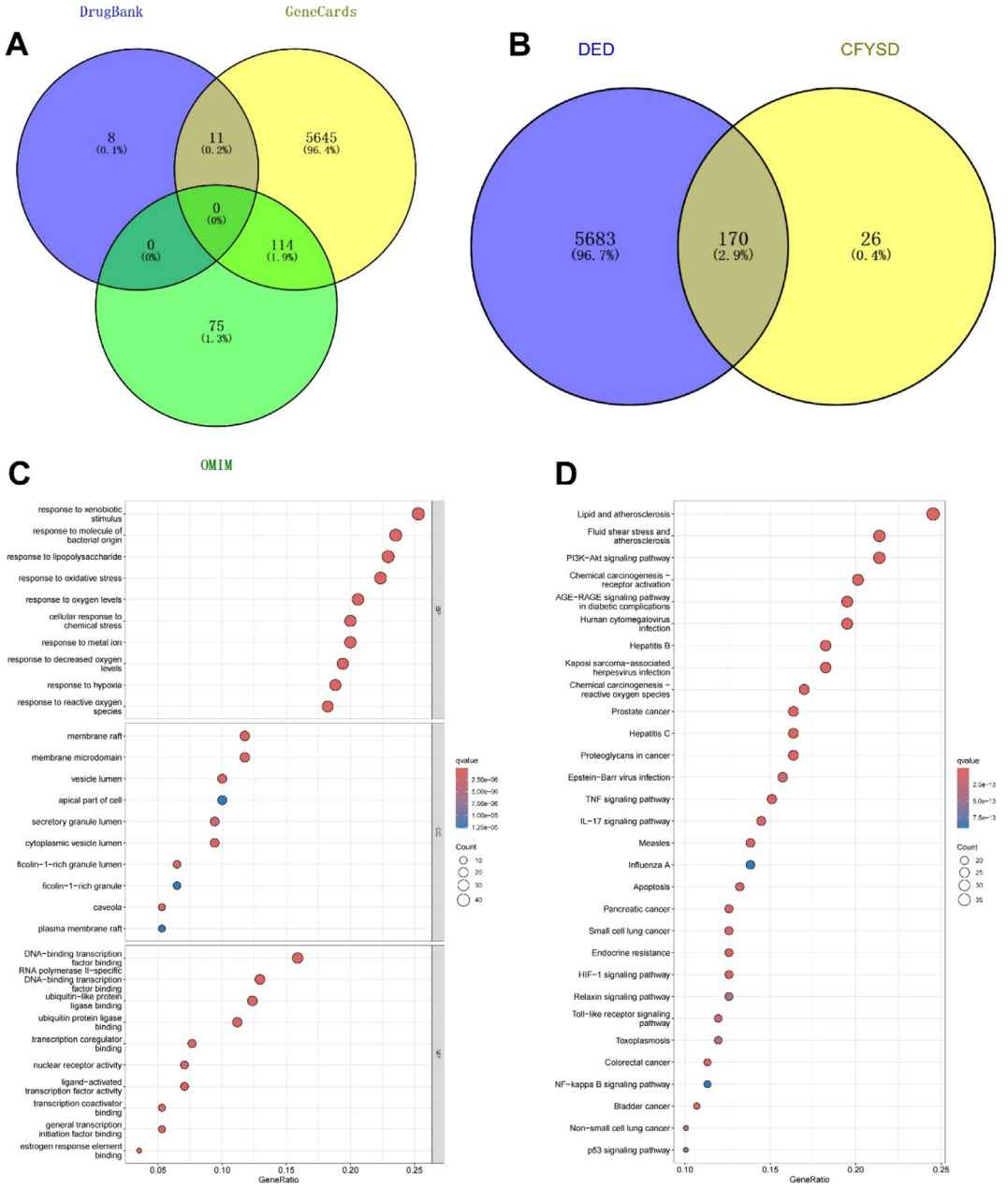

Fig. 1. Screening and enrichment analysis of target genes for CFYSD in treating DED. (A) Target genes related to DED in three databases; (B) Intersection of target genes between DED and CFYSD; (C) Bubble chart of GO enrichment analysis for candidate target genes, including the top 10 functional entries enriched in BP, CC, and MF; (D) Bubble chart of KEGG enrichment for candidate target genes, including the top 30 significantly enriched signaling pathways.

target genes were obtained (Fig. 1A and Table S2). The intersection of the predicted drug target genes and DED-related target genes was taken, and ultimately, 170 candidate target genes were retained (Fig. 1B). These 170 candidate target genes may be potential targets for CFYSD in treating DED.

To explore the functions of the above candidate target genes, GO and KEGG enrichment analyses on the 170 candidate target genes were performed. The GO enrichment analysis revealed that these candidate genes were mainly enriched in functional categories such as "response to xenobiotic stimulus", "membrane raft", and "DNA-binding transcription factor binding" (Fig. 1C, Fig. S1). The KEGG enrichment analysis indicated that these candidate genes were enriched in pathways such as "Lipid and atherosclerosis", "Fluid shear stress and atherosclerosis", and "PI3K/Akt" (Fig. 1D, Fig. S2). These pathways may be key pathways for CFYSD in the treatment of DED.

3.2. Identification of core ingredients and targets of CFYSD in treating DED

To further screen out the core targets from the candidate target genes mentioned above, the candidate target genes were uploaded to the STRING database for protein–protein interaction analysis (Fig. 2A, Fig. S3). Subsequently, the CytoHubba plugin was used to compute the degree, betweenness, and closeness of each gene in the protein interaction network to further refine the core targets (Table S3). The results showed that Akt1 and IL-1β ranked top in these three different centrality calculation methods, indicating that Akt1 and IL-1β play important regulatory roles in DED and may be the core targets for treating DED.

To further screen the core active ingredients of CFYSD in treating DED, a drug-active ingredient-target gene network was constructed using Cytoscape v3.8.0 software (Fig. 2B, Fig. S4).

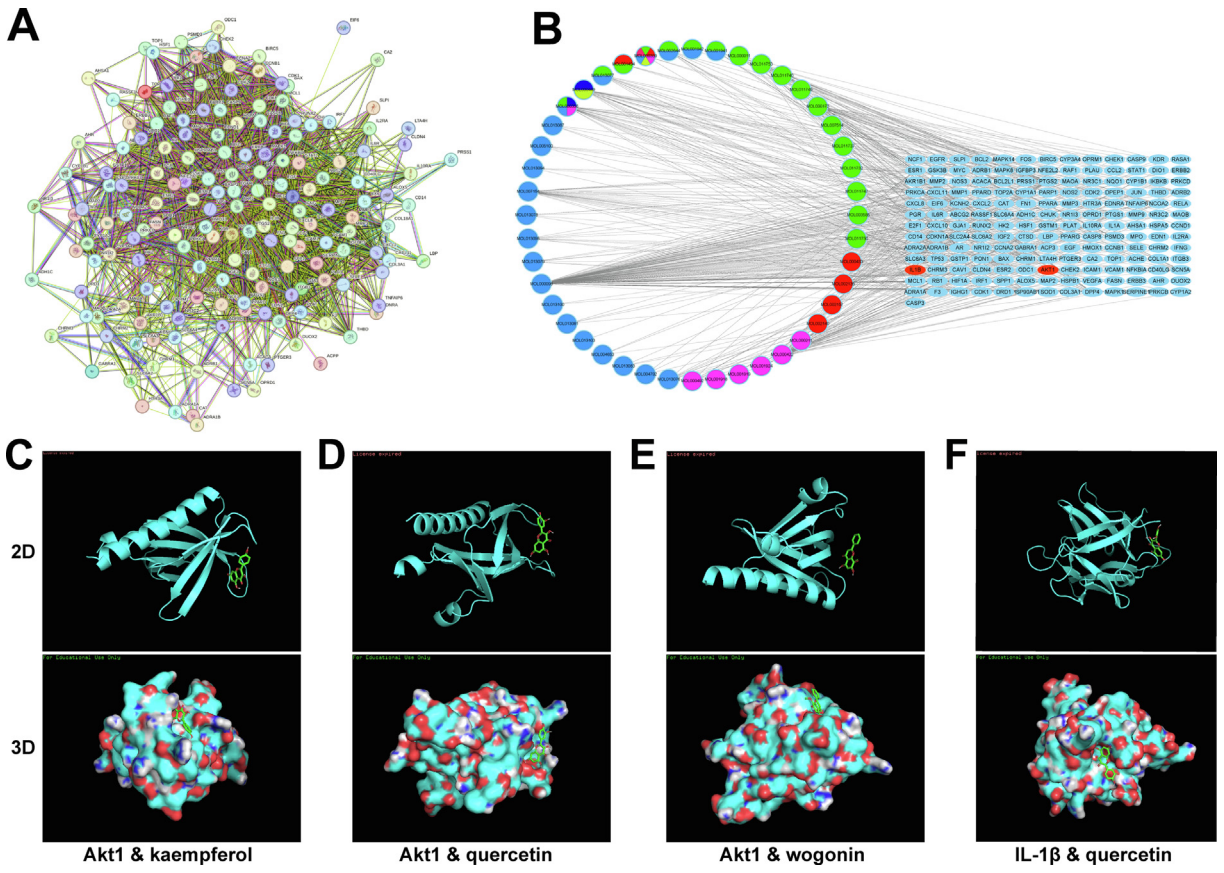

Fig. 2. Identification of core ingredients and targets of CFYSD in treating DED. (A) Protein interaction analysis of candidate target genes; (B) Network diagram of drug active ingredients and candidate target genes. The left side represents drug active ingredients, with different colors indicating that the active ingredients come from different drugs. The right side represents candidate target genes, and the lines between target genes and active ingredients indicate that the target genes may be regulated by the active ingredients. The red labels represent the core target genes identified in the screening process; (C) Molecular docking results of Akt1 with kaempferol molecule; (D) Molecular docking results of Akt1 with quercetin molecule; (E) Molecular docking results of Akt1 with wogonin molecule; (F) Molecular docking results of IL-1β with quercetin molecule. (For interpretation of the references to colour in this figure legend, the reader is referred to the web version of this article.)

Subsequently, potential target drugs for Akt1 and IL-1β were screened from the TCSMP database. The results indicated that Akt1 was targeted by kaempferol, wogonin, and quercetin, while IL-1β was targeted by quercetin, with kaempferol derived from Paeoniae Radix Alba, wogonin from Saposhnikoviae Radix, and quercetin from Peucedani Radix (Table S4). This suggests that Paeoniae Radix Alba, Saposhnikoviae Radix, and Peucedani Radix in CFYSD have a more significant impact on DED, and kaempferol, wogonin, and quercetin may be the core active ingredients for treating DED.

To investigate the interactions between core active components and core targets, molecular docking was used to simulate the binding interactions of Akt1 (1H10 | pdb_00001h10) and IL-1β (1HIB | pdb_00001hib) with kaempferol, wogonin, and quercetin. The results showed that kaempferol, wogonin, and quercetin exhibited good binding effects with Akt1 (Fig. 2C–F, Table 1), and quercetin showed good binding effects with IL-1β (Fig. S5, Fig. S6, Fig. S7, Fig. S8). This suggests that kaempferol, wogonin, and quercetin may exert therapeutic effects on DED by binding to Akt1 and IL-1β.

3.3. CFYSD alleviates hyperosmotic-induced HCE-T cell damage

Network pharmacology results indicated that CFYSD alleviates DED. To further validate this finding, HCE-T cells were treated with different concentrations of CFYSD (0.25, 0.5, 1, 2, 4 mg/mL), and no cytotoxic effects on HCE-T cells were found ($p > 0.05$, Fig. 3A). Next, HCE-T cells were exposed to hyperosmotic solution for 12 h, 24 h, and 48 h to establish an *in vitro* DED model, and then, different concentrations of CFYSD (0.25, 0.5, 1, 2, and 4 mg/mL) were added to the DED model. The results showed that HCE-T cell viability was remarkedly decreased after hyperosmotic induction ($p < 0.01$). Nevertheless, CFYSD restored cell viability in DED in a concentration-dependent manner ($p < 0.01$, Fig. 3B).

Based on the above results, HCE-T cells were treated with 1, 2, and 4 mg/mL CFYSD for 48 h for subsequent experiments. Results indicated that compared to the DED group, the higher dose group (1, 2, 4 mg/mL CFYSD) showed an obvious decrease in apoptosis rate ($p < 0.01$, Fig. 3C–D), as well as a significant reduction in the expression of IL-1β and TNF-α ($p < 0.01$, Fig. 3E). These results demonstrate that CFYSD can alleviate DED.

3.4. CFYSD alleviates DED by inhibiting the PI3K/Akt pathway

KEGG analysis indicated that the alleviative effects of CFYSD on DED may be associated with the PI3K/Akt pathway. To verify the effect of the PI3K/Akt pathway in CFYSD in treating DED, the expression of p-PI3K, PI3K, p-Akt, and Akt was measured by Western blot. The results showed that compared to the control group, the levels of p-PI3K/PI3K and p-Akt/Akt in the DED group were significantly increased ($p < 0.01$, Fig. 4A–B). Compared to the DED group, different concentrations (1, 2, 4 mg/mL) of CFYSD treatment

Table 1
Docking results between core targets and corresponding active components.

PDB ID	Resolution (A)	Compound	Structures	Binding energy (kcal/mol)
1H10	1.4	Akt1	kaempferol	−6.1
			quercetin	−6.1
			wogonin	−6.1
IHIB	2.4	IL-1β	quercetin	−7.9

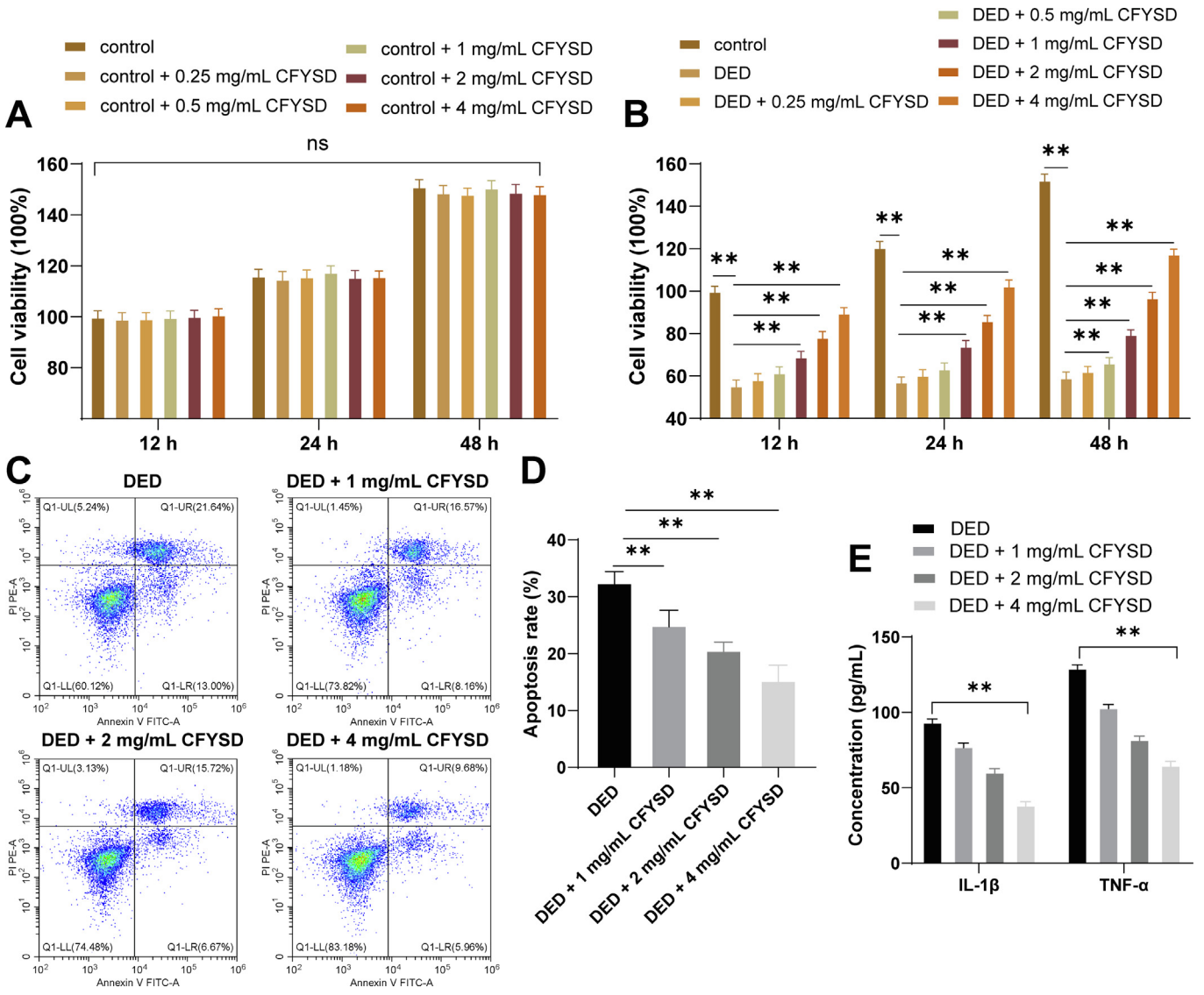

Fig. 3. CFYSD alleviates hyperosmotic-induced HCE-T cell damage. Different concentrations (0.25, 0.5, 1, 2, 4 mg/mL) of CFYSD were used to treat HCE-T cells, with blank group as control. (A) Cell viability was assessed using CCK-8 assay. Cells were treated with a hypertonic solution and then exposed to different concentrations (0.25, 0.5, 1, 2, 4 mg/mL) of CFYSD; (B) Cell viability was evaluated using CCK-8 assay. Cells were then treated with higher doses of CFYSD (1, 2, 4 mg/mL) for 48 h, with DED group as the control. (C) Cell apoptosis was detected using Annexin V-APC/PI. (D) Cell apoptosis rate was calculated. (E) IL-1β and TNF-α were measured using ELISA. The experiments were independently repeated three times, and the data are presented as mean ± standard deviation. Comparisons among multiple groups in panels A, B, and E were analyzed using two-way ANOVA, and in panel D were analyzed using one-way ANOVA, followed by Tukey's multiple comparisons test. * $p < 0.05$, ** $p < 0.01$.

significantly reduced the levels of p-PI3K/PI3K and p-Akt/Akt in cells ($p < 0.05$, Fig. 4A–B). These results indicate that CFYSD alleviates DED by inhibiting the activation of the PI3K/Akt pathway.

3.5. Activation of PI3K/Akt pathway reduces the alleviative effect of CFYSD on DED

To further verify that CFYSD treats DED through inhibiting the PI3K/Akt pathway, the PI3K activator 740 Y-P was added to the cells in the DED group and the DED + 4 mg/mL CFYSD group. Compared to cells without 740 Y-P treatment, the levels of p-PI3K/PI3K and p-Akt/Akt were significantly increased in cells treated with 740 Y-P ($p < 0.05$, Fig. 5A), cell viability was reduced ($p < 0.01$, Fig. 5B), cell apoptosis rate was increased ($p < 0.05$, Fig. 5C-D), and the expression of IL-1β and TNF-α was increased ($p < 0.01$, Fig. 5E). These results indicate that activation of the PI3K/Akt pathway reduces the effectiveness of CFYSD in alleviating DED.

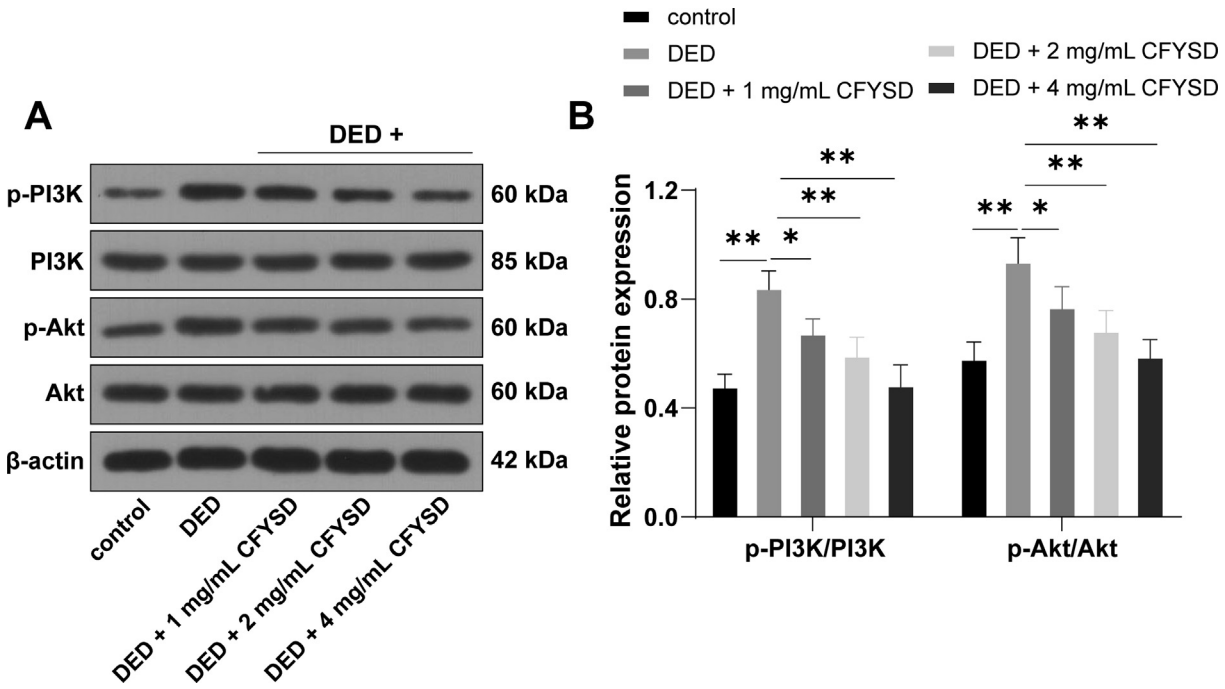

Fig. 4. CFYSD alleviates DED by inhibiting the PI3K/Akt pathway. HCE-T cells were exposed to a hypertonic solution for 48 h, followed by treatment with different concentrations (1, 2, 4 mg/mL) of CFYSD in a DED model for 48 h. (A) The expression of p-PI3K, PI3K, p-Akt, Akt, and β-actin was detected by Western blot; (B) The gray values of proteins were calculated. The experiments were independently repeated three times, and the data are presented as mean ± standard deviation. Comparisons among multiple groups in panel B were analyzed using two-way ANOVA, followed by Tukey's multiple comparisons test. * $p < 0.05$, ** $p < 0.01$.

4. Discussion

DED is a multifactorial disorder characterized by a complex pathological process involving oxidative stress, cell apoptosis, and inflammation [31]. However, current clinical drug therapies primarily target single pathological mechanism, resulting in limited treatment efficacy [32]. Our study proposed the potential of CFYSD as a treatment for DED and explored the targets and molecular mechanisms of CFYSD in treating DED through network pharmacology and experimental validation. With the results of the analyses, we hypothesized that CFYSD produces a therapeutic effect on DED by inhibiting the PI3K/Akt pathway.

In this study, drug target genes and DED-related target genes were screened through network pharmacology, and the intersection was taken to obtain 170 potential therapeutic target genes. The active ingredient-target gene network diagram showed that Akt1 and IL-1β are the core targets for treating DED and are regulated by kaempferol, wogonin, and quercetin. It has been documented that kaempferol is an anti-inflammatory agent that can inhibit IL-1β and TNF-α in human corneal epithelial cells in the DED model and repair damaged corneal epithelium [33]. Wogonin plays an antioxidative role in retinal diseases by reducing p-Akt and can protect cells from apoptosis [34]. Quercetin promotes the proliferation of corneal epithelial cells in DED models and downregulates the expression of p-PI3K, p-AKT, IL-6, and TNF-α, thus alleviating inflammation [12]. Moreover, molecular docking experiments have shown that kaempferol, wogonin, and quercetin act as the core active ingredients of CFYSD and exhibit good binding effects with Akt1 and IL-1β. Overall, CFYSD exerts therapeutic effects on DED mainly through the core active ingredients of kaempferol, wogonin, and quercetin, which may regulate Akt1 and IL-1β to participate in DED pathology.

Next, GO and KEGG enrichment analyses revealed that "Lipid and atherosclerosis", "Fluid shear stress and atherosclerosis", and "PI3K/Akt" may be key pathways for CFYSD in the treatment of DED. Therefore, we focused on the role of the PI3K/Akt pathway. After treating the DED cell model with CFYSD, cell viability was restored, cell apoptosis was reduced, and the levels of p-PI3K/PI3K and p-Akt/Akt were significantly decreased, indicating that the inhibition of the PI3K/Akt pathway may alleviate DED. Consistently, berberine eye drops treat DED by inhibiting the PI3K/AKT/NFκB and MAPK pathways and suppressing inflammatory cytokines to prevent cell apoptosis [13]. In DED animal models, treatment with DZ2002 alleviates conjunctival irritation and reduces corneal neovascularization and corneal opacity by inhibiting the activation of the STAT3-PI3K-Akt-NF-κB pathway [11]. Inhibiting the PTEN/PI3K/AKT pathway in a hyperosmotic-induced human corneal epithelial cell injury model can reduce the expression of IL-6 and TNF-α and thus reduce inflammation [12]. In conclusion, CFYSD achieves therapeutic effects on DED by restoring cell viability and reducing apoptosis via inhibition of the PI3K/Akt pathway.

There are several limitations in this study. Firstly, our study only elucidated the therapeutic mechanism of CFYSD on DED, without specifically investigating the role of the core active ingredients in treating DED. Secondly, animal experiments were not conducted for validation. Lastly, the therapeutic effect of CFYSD on DED required further verification through clinical trials. In future experiments, we will further investigate the mechanism of the core active ingredients in treating DED and perform additional clinical trials to explore the mechanism of action of CFYSD, providing new research directions for the treatment of DED.

In conclusion, this study proposed the core ingredients and targets of CFYSD for treating DED through pharmacological network

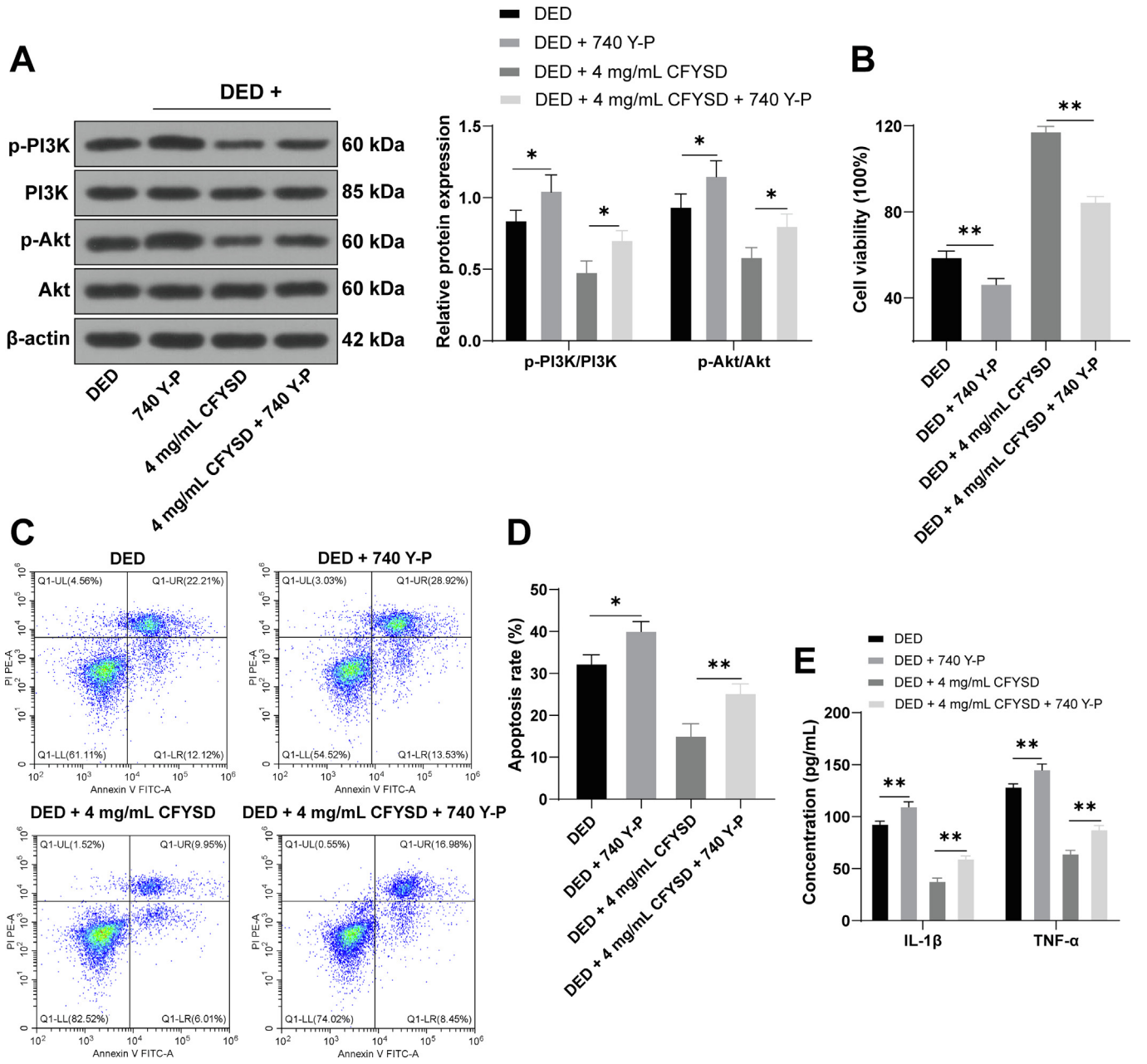

Fig. 5. Activation of PI3K/Akt pathway reduces the alleviative effect of CFYSD on DED. 740 Y-P was added to the DED group and DED + 4 mg/mL CFYSD group for 48 h, with no 740 Y-P treatment used as the control for the combined experiments. (A) The expression of p-PI3K, PI3K, p-Akt, Akt, and β-actin in the cells was detected by Western blot. (B) Cell viability was assessed using CCK-8 assay. (C) Cell apoptosis was detected using Annexin V-APC/PI. (D) Cell apoptosis rate was calculated. (E) The expression of IL-1β and TNF-α in the cells was measured by ELISA. The experiments were independently repeated three times, and the data were presented as mean ± standard deviation. Comparisons among multiple groups in panels A and E were analyzed using two-way ANOVA, and in panels B and E were analyzed using one-way ANOVA, followed by Tukey's multiple comparisons test. * $p < 0.05$, ** $p < 0.01$.

analysis and other experiments. CFYSD treats DED by inhibiting the activation of the PI3K/Akt pathway through multi-ingredients and multi-target mechanisms. Our findings may provide new evidence and research directions for the treatment of DED with CFYSD.

CRediT authorship contribution statement

Yue Du: Writing – original draft, Formal analysis, Conceptualization. **Xue Jiang:** Investigation, Writing – original draft. **Yanyan Zhang:** Project administration. **Quanyong Yi:** Writing – review & editing, Supervision, Funding acquisition.

Financial support

The research was funded by Health Science and Technology Plan Project of Ningbo (2022Y42). Medical and Health Science and Technology Plan Project of Zhejiang (2024KY367). Natural Science Foundation of Ningbo (2023J209).

Declaration of competing interest

The authors declare that they have no known competing financial interests or personal relationships that could have appeared to influence the work reported in this paper.

Supplementary material

https://doi.org/10.1016/j.ejbt.2025.05.006.

Data availability

Data will be made available on request.

References

[1] Mittal R, Patel S, Galor A. Alternative therapies for dry eye disease. Curr Opin Ophthalmol 2021;32(4):348–61. https://doi.org/10.1097/ICU.0000000000000768. PMid: 34010229.

[2] O'Neil EC, Henderson M, Massaro-Giordano M, et al. Advances in dry eye disease treatment. Curr Opin Ophthalmol 2019;30(3):166–78. https://doi.org/10.1097/ICU.0000000000000569. PMid: 30883442.

[3] Markoulli M, Hui A. Emerging targets of inflammation and tear secretion in dry eye disease. Drug Discov Today 2019;24(8):1427–32. https://doi.org/10.1016/j.drudis.2019.02.006. PMid: 30802601.

[4] Kojima T, Dogru M, Kawashima M, et al. Advances in the diagnosis and treatment of dry eye. Prog Retin Eye Res 2020;78:100842. https://doi.org/10.1016/j.preteyeres.2020.100842. PMid: 32004729.

[5] Mohamed HB, Abd El-Hamid BN, Fathalla D, et al. Current trends in pharmaceutical treatment of dry eye disease: A review. Eur J Pharm Sci 2022;175:106206. https://doi.org/10.1016/j.ejps.2022.106206. PMid: 35568107.

[6] Su SH, Ho TJ, Yang CC. Retrospective evaluation of the curative effect of traditional Chinese medicine on dry eye disease. Tzu Chi Med J 2021;33(4):365–439. https://doi.org/10.4103/tcmj.tcmj_281_20. PMid: 34760632.

[7] Lee TG, Hyun SW, Jo K, et al. *Achyranthis radix* extract improves urban particulate matter-induced dry eye disease. Int J Environ Res Public Health 2019;16(18):3229. https://doi.org/10.3390/ijerph16183229. PMid: 31487776.

[8] Liu P, Jiang P, Yu Y, et al. Modified Danzhi Xiaoyao Powder (MDXP) improves the corneal damage in dry eye disease (DED) mice through phagocytosis. J Ethnopharmacol 2024;321:117544. https://doi.org/10.1016/j.jep.2023.117544. PMid: 38070838.

[9] Chao WW, Tan SQ, Liu JH, et al. Dry eye: The effect of Chi-Ju-Di-Huang-Wan Plus Si Wu Tang and the underlying mechanism. J Altern Complement Med 2020;26(2):138–46. https://doi.org/10.1089/acm.2019.0201. PMid: 31651183.

[10] Sprogyte L, Park M, Di Girolamo N. Pathogenesis of alkali injury-induced limbal stem cell deficiency: A literature survey of animal models. Cells 2023;12(9):1294. https://doi.org/10.3390/cells12091294. PMid: 37174694.

[11] Wu CM, Mao JW, Zhu JZ, et al. DZ2002 alleviates corneal angiogenesis and inflammation in rodent models of dry eye disease via regulating STAT3-PI3K-akt-NF-κB pathway. Acta Pharmacol Sin 2024;45(1):166–79. https://doi.org/10.1038/s41401-023-01146-y. PMid: 37605050.

[12] Huang Y, Xia X, Li M, et al. Quercetin inhibits hypertonicity-induced inflammatory injury in human corneal epithelial cells via the PTEN/PI3K/AKT pathway. Tissue Cell 2024;89:102465. https://doi.org/10.1016/j.tice.2024.102465. PMid: 39024865.

[13] Han Y, Guo S, Li Y, et al. Berberine ameliorate inflammation and apoptosis via modulating PI3K/AKT/NFκB and MAPK pathway on dry eye. Phytomedicine 2023;121:155081. https://doi.org/10.1016/j.phymed.2023.155081. PMid: 37748390.

[14] Ru J, Li P, Wang J, et al. TCMSP: A database of systems pharmacology for drug discovery from herbal medicines. J Cheminform 2014;6:13. https://doi.org/10.1186/1758-2946-6-13. PMid: 24735618.

[15] Tian D, Gao Q, Chang Z, et al. Network pharmacology and *in vitro* studies reveal the pharmacological effects and molecular mechanisms of Shenzhi Jiannao prescription against vascular dementia. BMC Complement Med Ther 2022;22(1):33. https://doi.org/10.1186/s12906-021-03465-1. PMid: 35109845.

[16] Liu Y, Zhang J, Liu X, et al. Investigation on the mechanisms of guiqi huoxue capsule for treating cervical spondylosis based on network pharmacology and molecular docking. Medicine 2021;100(37):e26643. https://doi.org/10.1097/MD.0000000000026643. PMid: 34664825.

[17] Liu J, Liu J, Tong X, et al. Network pharmacology prediction and molecular docking-based strategy to discover the potential pharmacological mechanism of Huai Hua San against ulcerative colitis. Drug Des Devel Ther 2021;15:3255–76. https://doi.org/10.2147/DDDT.S319786. PMid: 34349502.

[18] Mok SR, Mohan S, Grewal N, et al. A genetic database can be utilized to identify potential biomarkers for biphenotypic hepatocellular carcinoma-cholangiocarcinoma. J Gastrointest Oncol 2016;7(4):570–9. https://doi.org/10.21037/jgo.2016.04.01. PMid: 27563447.

[19] Amberger JS, Bocchini CA, Schiettecatte F, et al. OMIM.org: Online Mendelian Inheritance in Man (OMIM®), an online catalog of human genes and genetic disorders. Nucleic Acids Res 2015;43(D1):D789–98. https://doi.org/10.1093/nar/gku1205. PMid: 25428349.

[20] Wishart DS, Feunang YD, Guo AC, et al. DrugBank 5.0: A major update to the DrugBank database for 2018. Nucleic Acids Res 2018;46(D1):D1074–82. https://doi.org/10.1093/nar/gkx1037. PMid: 29126136.

[21] Szklarczyk D, Gable AL, Nastou KC, et al. The STRING database in 2021: Customizable protein-protein networks, and functional characterization of user-uploaded gene/measurement sets. Nucleic Acids Res 2021;49(D1):D605–12. https://doi.org/10.1093/nar/gkaa1074. PMid: 33237311.

[22] Lu S, Sun X, Zhou Z, et al. Mechanism of Bazhen decoction in the treatment of colorectal cancer based on network pharmacology, molecular docking, and experimental validation. Front Immunol 2023;14:1235575. https://doi.org/10.3389/fimmu.2023.1235575. PMid: 37799727.

[23] Chen Z, Lin T, Liao X, et al. Network pharmacology based research into the effect and mechanism of Yinchenhao Decoction against Cholangiocarcinoma. Chin Med 2021;16(1):13. https://doi.org/10.1186/s13020-021-00423-4 PMid:33478536.

[24] ww PDB consortium. Protein Data Bank: The single global archive for 3D macromolecular structure data. Nucleic Acids Res 2019;47(D1):D520–8. https://doi.org/10.1093/nar/gky949. PMid: 30357364.

[25] Yuan S, Chan HCS, Filipek S, et al. PyMOL and inkscape bridge the data and the data visualization. Structure 2016;24(12):2041–2. https://doi.org/10.1016/j.str.2016.11.012. PMid: 27926832.

[26] Viegas DJ, Edwards TG, Bloom DC, et al. Virtual screening identified compounds that bind to cyclin dependent kinase 2 and prevent herpes simplex virus type 1 replication and reactivation in neurons. Antiviral Res 2019;172:104621. https://doi.org/10.1016/j.antiviral.2019.104621. PMid: 31634495.

[27] Kim S, Chen J, Cheng T, et al. PubChem 2023 update. Nucleic Acids Res 2023;51(D1):D1373–80. https://doi.org/10.1093/nar/gkac956. PMid: 36305812.

[28] Trott O, Olson AJ. AutoDock Vina: Improving the speed and accuracy of docking with a new scoring function, efficient optimization, and multithreading. J Comput Chem 2010;31(2):455–61. https://doi.org/10.1002/jcc.21334. PMid: 19499576.

[29] Li X, Chen C, Chen Y, et al. Oridonin ameliorates ocular surface inflammatory responses by inhibiting the NLRP3/caspase-1/GSDMD pyroptosis pathway in dry eye. Exp Eye Res 2024;245:109955. https://doi.org/10.1016/j.exer.2024.109955. PMid: 38843984.

[30] Li B, Liu J, Zhang D, et al. Evodiamine promotes autophagy and alleviates oxidative stress in dry eye disease through the p53/mTOR pathway. Invest Ophthalmol Vis Sci 2025;66(3):44. https://doi.org/10.1167/iovs.66.3.44. PMid: 40111353.

[31] Bu J, Liu Y, Zhang R, et al. Potential new target for dry eye disease-oxidative stress. Antioxidants 2024;13(4):422. https://doi.org/10.3390/antiox13040422. PMid: 38671870.

[32] Sheppard J, Shen Lee B, Periman LM. Dry eye disease: Identification and therapeutic strategies for primary care clinicians and clinical specialists. Ann Med 2023;55(1):241–52. https://doi.org/10.1080/07853890.2022.2157477. PMid: 36576348.

[33] Chen HC, Chen ZY, Wang TJ, et al. Herbal supplement in a buffer for dry eye syndrome treatment. Int J Mol Sci 2017;18(8):1697. https://doi.org/10.3390/ijms18081697. PMid: 28771187.

[34] Yan T, Bi H, Wang Y. Wogonin modulates hydroperoxide-induced apoptosis via PI3K/Akt pathway in retinal pigment epithelium cells. Diagn Pathol 2014;9:154. https://doi.org/10.1186/s13000-014-0154-3. PMid: 25432585.